European Congress on Computational Methods in Applied Sciences and Engineering
ECCOMAS 2000
Barcelona, 11-14 September 2000

AN EXTENDED FINITE ELEMENT METHOD (X-FEM) FOR TWO- AND THREE-DIMENSIONAL CRACK MODELING

N. Moës, N. Sukumar, B. Moran and T. Belytschko

Department of Mechanical and Civil Engineering, Northwestern University
2145 Sheridan Rd Evanston, IL 60208 USA
e-mail: moes@tam1.mech.nwu.edu, web page: http://www.tam.nwu.edu/X-FEM/

Key words: eXtended Finite Element Method, partition of unity, 3D fracture mechanics, stress intensity factors

Abstract. *The finite element method is now well established as a robust and reliable numerical technique in many areas of solid mechanics. There are however problems where the use of the finite element method is cumbersome like the modeling of moving discontinuities due to the need to update the mesh to match the geometry of the discontinuity. Even for stationary cracks, in three-dimensional solids, contsructing a mesh that matches the geometry of the crack is not trivial for non-symmetric loading cases. Recently, a new technique for modeling cracks in the finite element framework has been introduced. A standard displacement-based approximation is enriched near a crack by incorporating both a discontinuous field and the near crack front asymptotic fields through a partition of unity method. A methodology that constructs the enriched approximation from the interaction of the crack geometry with the mesh is developed. This technique allows the entire crack to be represented independently of the mesh, and so remeshing is not necessary to model crack growth. Numerical experiments are provided to demonstrate the utility and robustness of the proposed technique. Two-dimensional crack growth analysis are shown and stress intensity factors for planar three-dimensional crack obtained with the X-FEM are compared to available reference solutions from the literature.*

1 INTRODUCTION

Solving crack problems in fracture mechanics is imperative to quantify and predict the behavior of cracked structures under service conditions. To this end, the accurate evaluation of fracture parameters such as the stress intensity factors (SIF) is required for simulation-based life-cycle design analysis.

The modeling of cracks using the finite element method is cumbersome in 3D for complex structures or crack geometries. Even in 2D, fatigue crack growth is not a straightforward task. The present technique, the eXtended Finite Element Method, models cracks independently of the mesh leading to a simplification in mesh generation and avoiding remeshing as the crack grows.

The X-FEM exploits the partition of unity property of finite elements first identified in [?], which allows local enrichment functions to be easily incorporated into a finite element approximation. A standard approximation is thus "enriched" in a region of interest by the local functions in conjunction with additional degrees of freedom. The enrichment functions are the near-tip asymptotic fields [?] and a discontinuous function [?] to represent the jump in displacement across the crack boundary. The extension to the 3D case was carried out in [?]. The use of the partition of unity method in conjunction with the finite element method to model cracks may also be found in [?] and [?].

The paper is organized as follows. The next section is devoted to the description of the strong and weak forms of the elasto-statics equations in the presence of cracks. Then, Section 3 introduces the X-FEM approximation in both two and three dimensions. Section 4 presents a 2D crack growth numerical experiment as well as the determination of the stress intensity factors for an elliptical crack. Finally, Section 5 provides a summary and some concluding remarks.

2 PROBLEM FORMULATION

In this section, we briefly review the governing equations for elasto-statics and give the associated weak form. Specifically, we consider the case when an internal boundary is present across which the displacement field may be discontinuous. The internal boundary is a curve in two-dimensional problems and a surface in three-dimensional problems.

2.1 Governing equations

Consider the domain Ω bounded by Γ. The boundary Γ is composed of the sets Γ_u, Γ_t, and Γ_c, such that $\Gamma = \Gamma_u \cup \Gamma_t \cup \Gamma_c$ as shown in Fig. ??. The crack is located on Γ_c and is assumed to be traction-free. Prescribed displacements are imposed on Γ_u, while tractions are imposed on Γ_t.

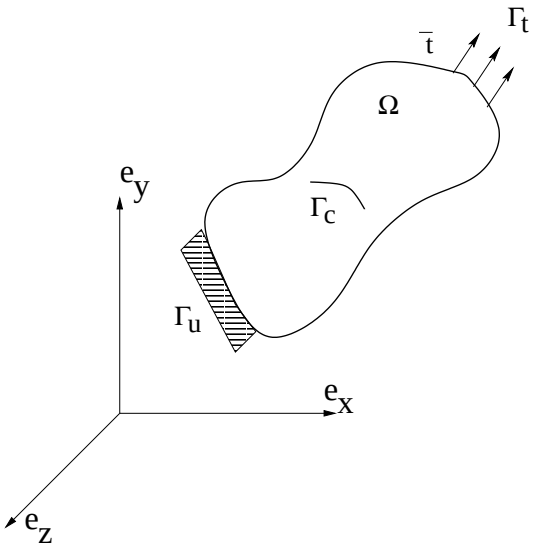

Figure 1: Body with an internal boundary subjected to loads.

The equilibrium equations and boundary conditions are

$$\boldsymbol{\nabla} \cdot \boldsymbol{\sigma} + \boldsymbol{b} = 0 \quad \text{in} \quad \Omega \tag{1}$$

$$\boldsymbol{\sigma} \cdot \boldsymbol{n} = \overline{\boldsymbol{t}} \text{ on } \Gamma_t \tag{2}$$

$$\boldsymbol{\sigma} \cdot \boldsymbol{n} = 0 \text{ on } \Gamma_{c+} \tag{3}$$

$$\boldsymbol{\sigma} \cdot \boldsymbol{n} = 0 \text{ on } \Gamma_{c-} \tag{4}$$

where Γ_{c+} and Γ_{c-} are the crack faces, $\boldsymbol{n}$ the unit outward normal, $\boldsymbol{\sigma}$ the Cauchy stress, and $\boldsymbol{b}$ the body force per unit volume. In the present investigation, we consider small strains and displacements. The kinematics equations therefore consist of the strain-displacement relation

$$\boldsymbol{\epsilon} = \boldsymbol{\epsilon}(\boldsymbol{u}) = \boldsymbol{\nabla}_s \boldsymbol{u} \tag{5}$$

where $\boldsymbol{\nabla}_s$ is the symmetric part of the gradient operator, and the essential boundary conditions

$$\boldsymbol{u} = \overline{\boldsymbol{u}} \text{ on } \Gamma_u \tag{6}$$

The constitutive relation is given by Hooke's law:

$$\boldsymbol{\sigma} = \boldsymbol{C} : \boldsymbol{\epsilon} \tag{7}$$

where $\boldsymbol{C}$ is the Hooke tensor.

2.2 Weak form

The space of admissible displacement fields is defined by

$$\mathcal{U} = \{\boldsymbol{v} \in \mathcal{V} : \boldsymbol{v} = \overline{\boldsymbol{u}} \text{ on } \Gamma_u\} \tag{8}$$

where the space $\mathcal{V}$ is related to the regularity of the solution. The details on this matter when the domain contains an internal boundary or re-entrant corner may be found in [?] and [?]. The test function space is defined similarly as

$$\mathcal{U}_0 = \{\boldsymbol{v} \in \mathcal{V} : \boldsymbol{v} = 0 \text{ on } \Gamma_u\} \tag{9}$$

An important point to note is that the space $\mathcal{V}$ allows the trial and test functions to be discontinuous across the internal boundary Γ_c. The weak form of the equilibrium equations is given by

$$\int_\Omega \boldsymbol{\sigma} : \boldsymbol{\epsilon}(\boldsymbol{v}) \ \mathrm{d}\Omega = \int_\Omega \boldsymbol{b} \cdot \boldsymbol{v} \ \mathrm{d}\Omega + \int_{\Gamma_t} \overline{\boldsymbol{t}} \cdot \boldsymbol{v} \ \mathrm{d}\Gamma \ \forall \ \boldsymbol{v} \in \mathcal{U}_0 \tag{10}$$

Using the constitutive relation and the kinematics constraints in the weak form, the problem is to find $\boldsymbol{u} \in \mathcal{U}$ such that

$$\int_\Omega \boldsymbol{\epsilon}(\boldsymbol{u}) : \boldsymbol{C} : \boldsymbol{\epsilon}(\boldsymbol{v}) \ \mathrm{d}\Omega = \int_\Omega \boldsymbol{b} \cdot \boldsymbol{v} \ \mathrm{d}\Omega + \int_{\Gamma_t} \overline{\boldsymbol{t}} \cdot \boldsymbol{v} \ \mathrm{d}\Gamma \ \forall \ \boldsymbol{v} \in \mathcal{U}_0 \tag{11}$$

The above weak form is equivalent to the strong form (??)-(??) (see [?]). In particular, the fact that the test function $\mathcal{V}$ may be discontinuous across Γ_c yields the traction free conditions on the crack faces (??)-(??).

3 THE EXTENDED FINITE ELEMENT METHOD

In this section, we develop the approximation associated to the weak form (??). The extended finite element approximation involves two terms: the classical finite element approximation on the given mesh and an enriched finite element approximation obtained through the partition of unity method [?]. The enrichment takes into account the displacement discontinuity induced by the crack as well as the analytical asymptotic behavior near the crack front.

3.1 Two-dimensional case

Consider Fig. ?? in which a crack is not modeled by the finite element mesh. The extended finite element approximation introduced in [?, ?] takes the form:

$$\begin{aligned} \boldsymbol{u}^h(\boldsymbol{x}) &= \sum_{i \in I} \boldsymbol{u}_i \phi_i(\boldsymbol{x}) + \sum_{i \in L} \boldsymbol{a}_i \phi_i(\boldsymbol{x}) H(\boldsymbol{x}) \\ &+ \sum_{i \in K_1} \phi_i(\boldsymbol{x}) (\sum_{l=1}^{4} \boldsymbol{b}_{i,1}^l F_1^l(\boldsymbol{x})) + \sum_{i \in K_2} \phi_i(\boldsymbol{x}) (\sum_{l=1}^{4} \boldsymbol{b}_{i,2}^l F_2^l(\boldsymbol{x})) \end{aligned} \tag{12}$$

where:

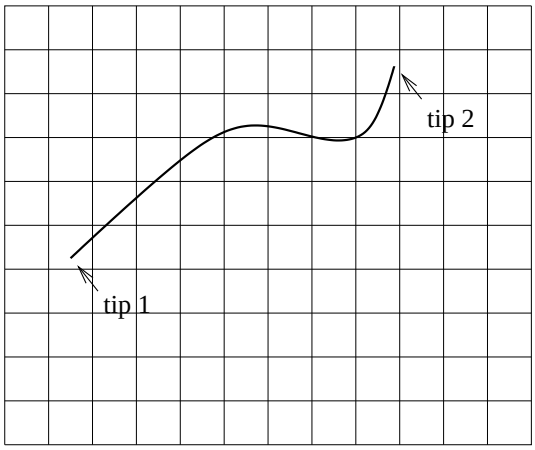

Figure 2: An arbitrary crack placed on a mesh.

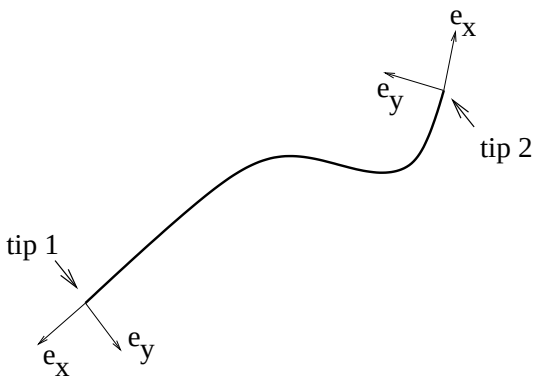

Figure 3: Local axes for the polar coordinates at the two crack tips.

- I is the set of all nodes in the mesh;
- $\boldsymbol{u}_i$ is the classical (vectorial) degree of freedom at node i;
- ϕ_i is the shape function associated with node i. Each shape function ϕ_i has compact support ω_i given by the union of the elements connected to node i;
- $L \subset I$ is the subset of nodes that are enriched for the crack discontinuity and $\boldsymbol{a}_i$ are the corresponding additional degrees of freedom; the nodes in L are such that their support (we mean the support of the nodal shape function) intersects the crack but do not contain any of its two tips. They are shown as circled nodes (Fig. **??**) on a uniform or non-uniform mesh;
- $K_1 \subset I$ and $K_2 \subset I$ are the subset of nodes that are enriched for the first and second crack tip, respectively. The corresponding additional degrees of freedom are $\boldsymbol{b}^l_{i,1}$ and $\boldsymbol{b}^l_{i,2}$; the nodes in K_1 (K_2) are such that their support contain the first (second) crack tip. The squared nodes Fig. **??** belongs to $K_1 \cup K_2$.

The near tip functions $F^l_1(\boldsymbol{x}), l = 1, \ldots, 4$ are given by

$$\{F^l_1(\boldsymbol{x})\} \equiv \left\{ \sqrt{r}\sin(\frac{\theta}{2}), \sqrt{r}\cos(\frac{\theta}{2}), \sqrt{r}\sin(\frac{\theta}{2})\sin(\theta), \sqrt{r}\cos(\frac{\theta}{2})\sin(\theta) \right\} \tag{13}$$

where (r, θ) are the local polar coordinates at the first crack tip with $\theta = 0$ coinciding with the tangent to the crack at the tip. Similarly, the near tip functions $F^l_2(\boldsymbol{x})$ are also given by (**??**) but the local polar coordinates being now defined at the second crack tip. Fig. **??** shows the local axes for the definition of the polar coordinates at the two crack tips.

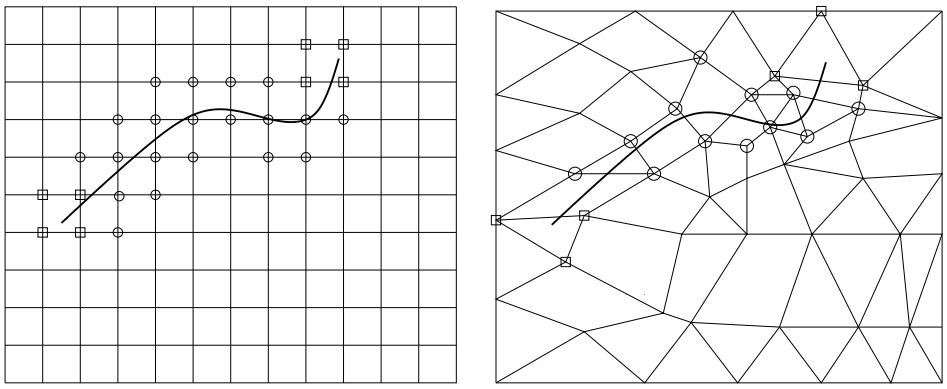

Figure 4: Crack on a uniform mesh (left) and on a non uniform mesh (right). The circled nodes belong to the set L and are enriched by the jump function whereas the squared nodes belong to the set $K_1 \cup K_2$ and are enriched by the crack tip functions.

The function $H(\boldsymbol{x})$ is a discontinuous function across the crack surface and is constant on each side of the crack: +1 on one side of the crack and -1 on the other. More precisely, the function $H(\boldsymbol{x})$ is defined as follows. The crack is considered to be a curve parametrized by the curvilinear coordinate s, as in Fig. **??**. Given a point $\boldsymbol{x}$ in the domain, we denote by $\boldsymbol{x}^*$ the closest point on the crack to $\boldsymbol{x}$. At $\boldsymbol{x}^*$, we construct the tangent and normal vector to the curve, $\boldsymbol{e}_s$ and $\boldsymbol{e}_n$, with the orientation of $\boldsymbol{e}_n$ taken such that $\boldsymbol{e}_s \times \boldsymbol{e}_n = \boldsymbol{e}_z$ where the unit vector $\boldsymbol{e}_z$ points out of the page. The function $H(\boldsymbol{x})$ is then given by the sign of the scalar product $(\boldsymbol{x} - \boldsymbol{x}^*) \cdot \boldsymbol{e}_n$. In the case of a kinked crack as shown in Fig. **??**b, where no unique normal exists but a cone of normals is defined at $\boldsymbol{x}^*$, $H(\boldsymbol{x}) = 1$ if the vector $(\boldsymbol{x} - \boldsymbol{x}^*)$ belongs to the cone of normals at $\boldsymbol{x}^*$ and $H(\boldsymbol{x}) = -1$ otherwise.

3.2 Three-dimensional case

The three-dimensional case is treated quite similarly to the two-dimensional case except that now the front of the crack is no longer composed of a set of points but a set of curves. The set K now gathers all the nodes to be enriched to model the crack front and the approximation reads [**?**]

$$\begin{aligned} \boldsymbol{u}^h(\boldsymbol{x}) &= \sum_{i \in I} \boldsymbol{u}_i \phi_i(\boldsymbol{x}) + \sum_{i \in L} \boldsymbol{a}_i \phi_i(\boldsymbol{x}) H(\boldsymbol{x}) \\ &+ \sum_{i \in K} \phi_i(\boldsymbol{x}) \Big(\sum_{l=1}^{4} \boldsymbol{b}_i^l F^l(\boldsymbol{x}) \Big) \end{aligned} \tag{14}$$

where I, $\boldsymbol{u}_i$, ϕ_i have the same meaning as before, whereas the sets L and K are given by

- $L \subset I$ is the subset of nodes that are enriched for the crack discontinuity and $\boldsymbol{a}_i$ are the corresponding additional degrees of freedom; the nodes in L are such that their

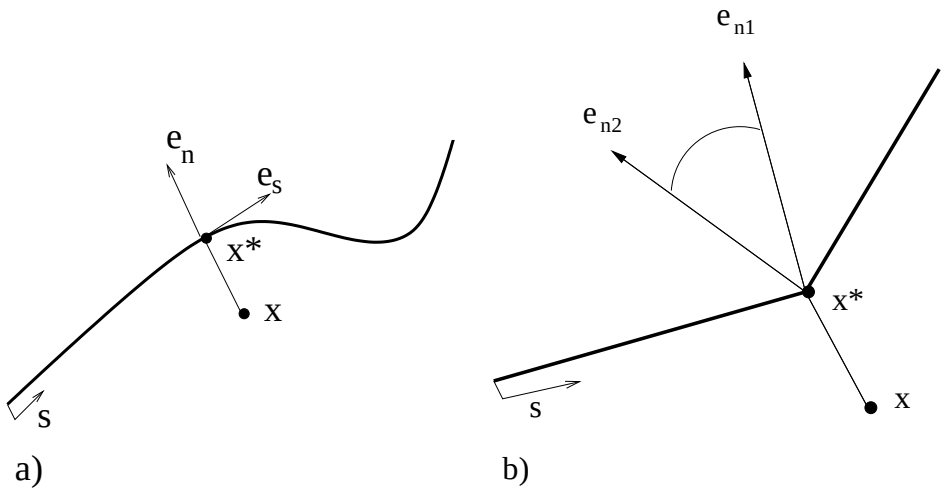

Figure 5: Normal and tangential coordinates for a smooth crack, (a), and a kinked crack, (b). $\boldsymbol{x}^*$ is the closest point to $\boldsymbol{x}$ on the crack. The value of the function H is -1 at $\boldsymbol{x}$ for (a) and (b).

support intersects the crack but not its front. Note that the support of a node is now a volume;

- $K \subset I$ the subset of nodes that are enriched for the front. The corresponding additional degrees of freedom are $\boldsymbol{b}_i^l$, $l = 1, \ldots, 4$, the nodes in K are such that their support intersects the front.

The front enrichment functions $F^l(\boldsymbol{x})$ are still given by (??) where the couple (r, θ) is defined as the polar coordinates in the $x_{\hat{1}} - x_{\hat{2}}$ plane, see Fig. ??. The plane $x_{\hat{1}} - x_{\hat{2}}$ contains $\boldsymbol{x}$ and $\boldsymbol{x}^*$ (the closest point on the crack front to $\boldsymbol{x}$) and the $x_{\hat{2}}$ axis is aligned with the normal $\boldsymbol{n}$ to the crack at $\boldsymbol{x}^*$.

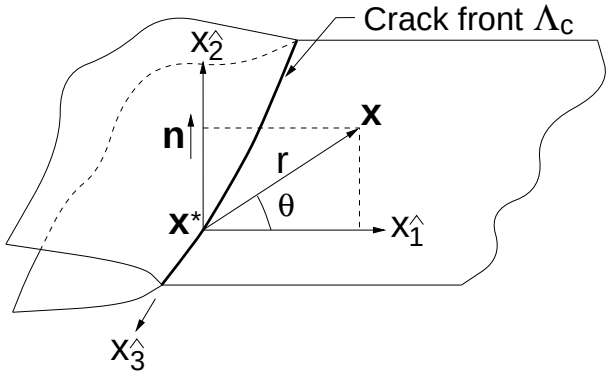

Figure 6: Coordinate configuration for crack front enrichment functions.

The crack discontinuity enrichment function $H(\boldsymbol{x})$ is still +1 above the crack and -1 below. The 2D definition of $H(\boldsymbol{x})$ depicted in Fig.?? may directly be generalized to 3D.

3.3 Implementation aspects

The cracks are modeled by a set of geometrical entities. The simplest is to use segments in 2D and planar surfaces in 3D as geometrical entities. To determine whether a point $\boldsymbol{x}$ is above or below the crack and to evaluate $H(\boldsymbol{x})$, we find the geometrical entity the point $\boldsymbol{x}$ is closest to and compute the signed convex area (2D) or volume (3D) enclosed by the point and the entity. The sign of this area or volume determines whether the point is above or below the crack.

For elements cut by the crack and enriched with the jump function $H(\boldsymbol{x})$, it is necessary to make a modification to the element quadrature routines in order to accurately assemble the contribution to the weak form on both sides of the discontinuity. As the crack is allowed to be arbitrarily oriented in an element, the use of standard Gauss quadrature may not adequately integrate the discontinuous field. If the integration of the jump enrichment is indistinguishable from that of a constant function, spurious singular modes can appear in the system of equations. In order to avoid this situation, an element cut by the crack is decomposed into simplexes all being on one side or the other of the crack. The integration is then performed by first looping over these simplexes and then the integration points in each simplex.

4 NUMERICAL EXPERIMENTS

4.1 Crack growth from two holes

We consider the modeling of crack growth in a plate with cracks emanating from two holes subjected to a far-field uniform tension. Fig. ?? shows the geometry and loads under consideration. In the initial configuration, both cracks have a length of 0.1 `in.` and are oriented at angles $\theta = 45°$ and $\theta = -45°$ for the left and right holes, respectively. The mesh used in the analysis is also shown in Fig. ?? (2650 nodes). It is refined towards the center of the plate, where the cracks are expected to propagate. It is emphasized that the mesh does not conform to the crack geometries, and that the same mesh is used throughout the simulation.

The cracks are driven by a Paris fatigue law with the maximum circumferential stress hypothesis used to determine the angle of crack propagation. The change in crack length for each iteration is taken to be a constant $\Delta a = 0.05$ `in.`, and the cracks are grown for 16 steps. The two cracks grow in a nearly symmetrical pattern, despite the fact that the mesh is not symmetric (see Fig. ?? and a zoom around the right hole which is shown in Fig. ??). In this example, the cracks eventually grow into the holes. See [?] for more details on this numerical experiment.

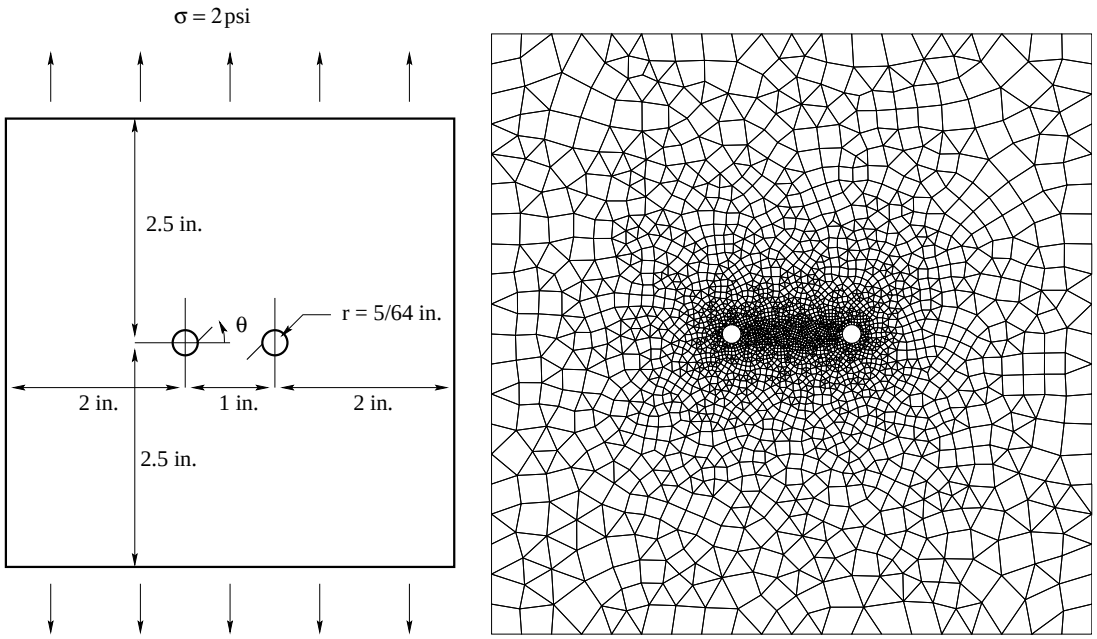

Figure 7: Description and mesh for the crack growth problem. The initial crack lengths are 0.2 `in`.

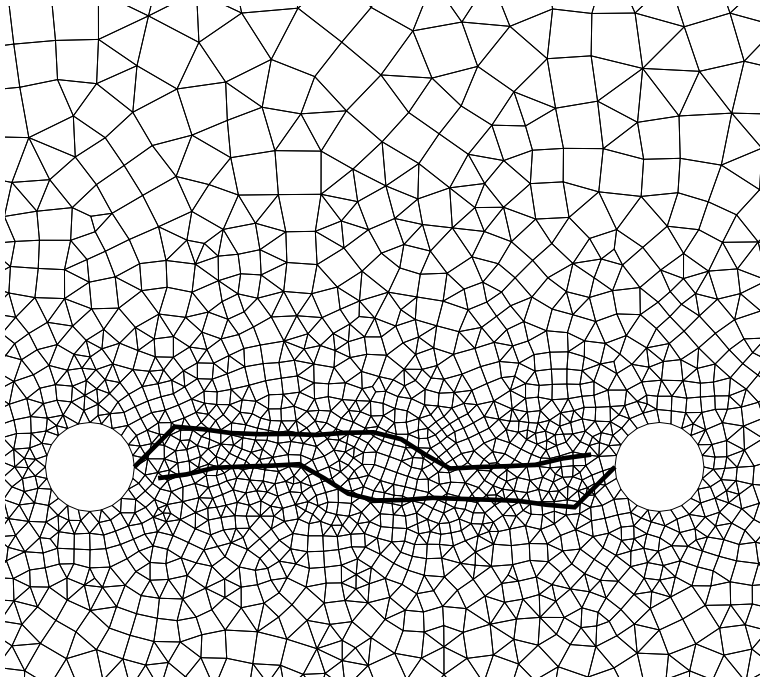

Figure 8: Mesh and final crack configuration.

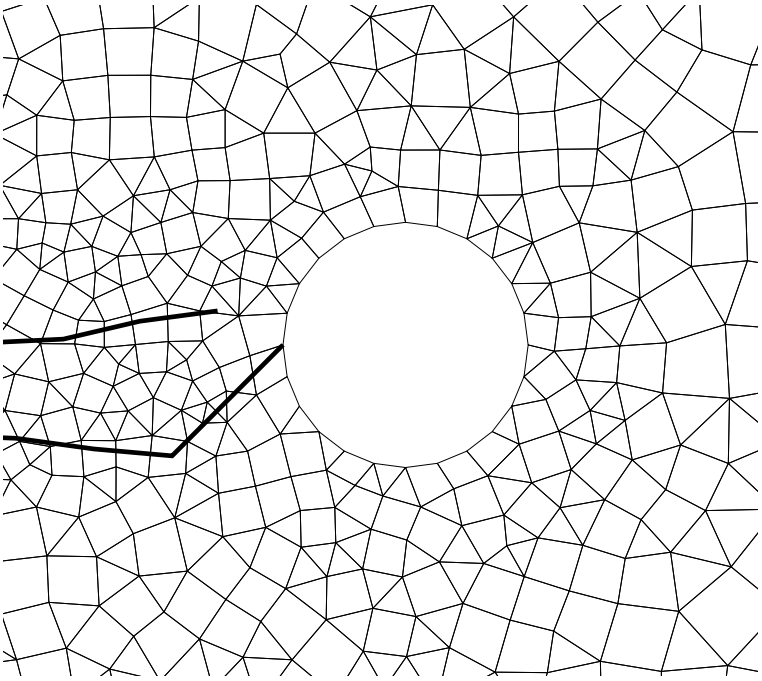

Figure 9: Mesh and final crack configuration near the right hole.

4.2 Elliptical crack

We consider an elliptical crack with semi-major axis $a = 0.1$ and semi-minor axis $b = 0.05$ inside a bi-unit cube. The body is subjected to unit tractions $\sigma^0_{33} = 1$ on $x_3 = \pm 1$. The coordinate axis x_3 is normal to the plane of the crack. Since the crack-dimensions are small compared to the specimen, we use the infinite domain solution as the reference solution. The exact stress intensity factor solution for a planar elliptical crack in an infinite domain is [**?**]:

$$K_I^E = \frac{\sigma^0_{33}\sqrt{\pi b}}{E(k)} \left\{ \sin^2\theta + \frac{b^2}{a^2}\cos^2\theta \right\}^{\frac{1}{4}}, \tag{15}$$

where θ is the elliptic angle defined Fig. **??**, σ^0_{33} is the far-field applied stress in the x_3-direction, and $E(k)$ which is the elliptic integral of the second kind is given by

$$E(k) = \int_0^{\pi/2} \sqrt{1 - k^2 \sin^2\theta}\, d\theta, \quad k^2 = \frac{a^2 - b^2}{a^2}. \tag{16}$$

The finite element mesh consists of $24 \times 24 \times 24$ hexahedral elements. The number of unknowns in the matrix system is 48324. The stress intensity factors (SIF) are computed

in a post-processing step using domain integral methods [?]. The SIF results have four-fold symmetry; hence results for only $0° \leq \theta \leq 90°$ are presented. For the chosen values of a and b, the value of the elliptic integral $E(k) = 1.211096$ [?]. In Table ??, the SIF results are presented as a function of the elliptic angle θ, and Fig. ??, the normalized SIF is plotted versus θ. The agreement between the exact solution and the numerical results is good for the entire range of θ. The minimum ($\theta = 10°$) and maximum ($\theta = 30°$) errors in the stress intensity factors are 0.6 per cent and 3.7 per cent, respectively. More details on this problem as well as other examples with penny-shaped and edge cracks can be found in [?].

5 CONCLUSIONS

The eXtended Finite Element Method allows the representation of cracks independent of the mesh As a consequence no remeshing is necessary for the crack growth simulation. On the basis of the Paris fatigue law, the growth of two cracks emanating from a hole was analyzed in a two-dimensional problem on a fixed mesh. For the three-dimensional case, accurate stress intensity factors were obtained for an elliptical crack using a uniform hexahedral mesh.

Table 1: Stress intensity factors for the elliptical crack problem.

θ	K_I^E	K_I
0°	0.2314	0.2358
10°	0.2365	0.2378
20°	0.2495	0.2459
30°	0.2662	0.2564
40°	0.2830	0.2776
50°	0.2983	0.2965
60°	0.3107	0.3089
70°	0.3198	0.3163
80°	0.3253	0.3194
90°	0.3273	0.3202

REFERENCES

[1] I. Babuška and M. Rosenzweig. A finite element scheme for domains with corners. *Numer. Math.*, 20:1–21, 1972.

[2] T. Belytschko and T. Black. Elastic crack growth in finite elements with minimal remeshing. *International Journal of Numerical Methods in Engineering*, 45(5):601–620, 1999.

[3] R. F. Byrd and M. D. Friedman. *Handbook of Elliptic Integrals for Engineers & Scientists*. Springer-Verlag, Berlin, 1971.

[4] C. A. Duarte, O. N. Hamzeh, T. J. Liszka, and W. W Tworzydlo. The element partition method for the simulation of three-dimensional dynamic crack propagation. *Computer Methods in Applied Mechanics and Engineering*, 1999. submitted.

[5] P. Grisvard. *Elliptic Problems in Nonsmooth Domains*. Pitman Publishing, Inc, Boston, 1985.

[6] G. R. Irwin. The crack extension force for a part-through crack in a plate. *ASME, Journal of Applied Mechanics*, 29:651–654, 1962.

[7] J. M. Melenk and I. Babuška. The partition of unity finite element method: Basic theory and applications. *Computer Methods in Applied Mechanics and Engineering*, 39:289–314, 1996.

[8] N. Moës, J. Dolbow, and T. Belytschko. A finite element method for crack growth without remeshing. *International Journal of Numerical Methods in Engineering*, 46:131–150, 1999.

[9] T. Strouboulis, I. Babuška, and K. Copps. The design and analysis of the generalized finite element method. *Computer Methods in Applied Mechanics and Engineering*, 181:43–71, 2000.

[10] N. Sukumar, N. Moës, T. Belytschko, and B. Moran. Extended Finite Element Method for three-dimensional crack modeling. *International Journal of Numerical Methods in Engineering*, 1999. Accepted.

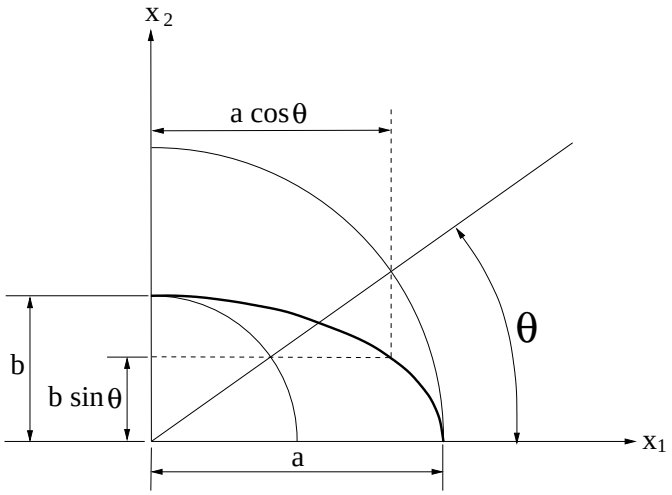

Figure 10: Geometric definitions for an elliptical crack.

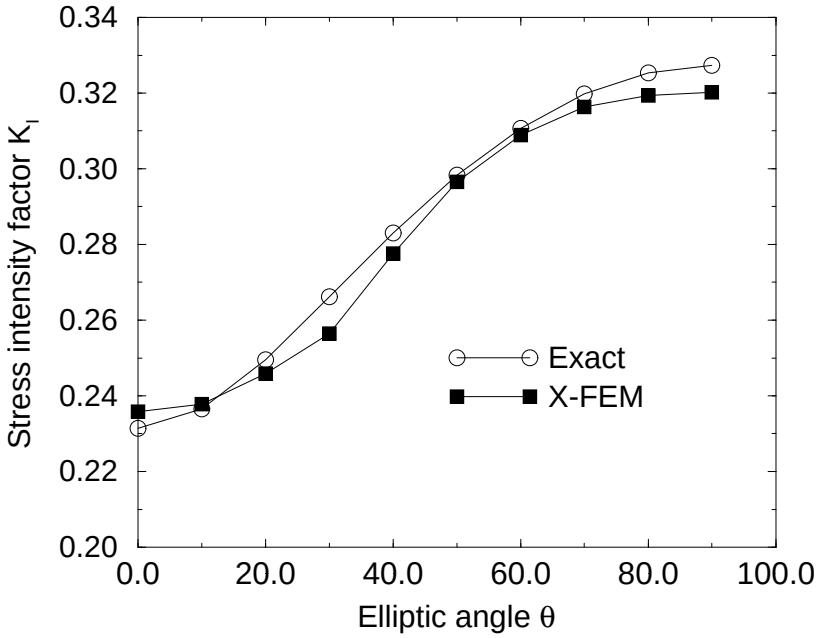

Figure 11: Stress intensity factors for the elliptical crack problem.